JOURNAL OF GUIDANCE, CONTROL, AND DYNAMICS
Vol. 18, No. 3, May–June 1995

Structural Damage Detection Using Constrained Eigenstructure Assignment

Tae W. Lim*
University of Kansas, Lawrence, Kansas 66045

System health monitoring of aerospace vehicles is important not only for conducting safe operation but also for maintaining system performance. Structural health along with sensor and actuator malfunction must be monitored to perform the system health monitoring. As a step toward developing a system health monitoring scheme, this paper investigates structural damage detection using a constrained eigenstructure assignment. The eigenstructure assignment is selected for the investigation since it may be used not only to perform structural damage detection but also to monitor the sensor and actuator performance in a unified manner. To employ the eigenstructure assignment in the framework of structural modeling and modal testing, a concept of constrained eigenstructure assignment is developed. The constrained eigenstructure assignment makes it possible that the computed feedback gains correspond directly to the structural parameter changes. To demonstrate the capability of the approach, a 20-bay planar truss structure is employed. Modal tests are performed using 11 accelerometers for the undamaged structure and several missing member damage cases. Then the test modes are used to locate the missing member. In spite of incomplete mode shapes and test inaccuracies, accurate damage detection is conducted.

Introduction

ENVISIONED future spacecraft are expected to be assembled on-orbit to achieve necessary size while maintaining acceptable launch economy. Although larger and more complex than their predecessors, they must meet stringent attitude, pointing, and shape control requirements to support precision scientific instruments and payloads on board.[1] Distributed sensors and actuators are expected to be employed to meet the performance requirements for the flexible spacecraft. To achieve the desired performance, accurate mathematical modeling and verification of structural dynamic characteristics are essential. Also, to maintain the performance during the expected lifetime of the spacecraft, the integrity or the health of the spacecraft needs to be monitored periodically. The structural damage detection method investigated in this paper is based on the idea that system performance changes resulting from structural damage can be quantified by measuring eigenvalues and eigenvectors. In other words, eigenvalues and eigenvectors are monitored periodically to detect significant changes, and they are used to locate structural damage.

Numerous researchers have studied structural damage location methods using modal test data. These methods can be classified based on the ways of defining the structural model and design parameters, utilizing the experimental data, and estimating the parameters. The class of methods that has been explored most widely is known as optimal matrix update. The goal of the optimal matrix update is to seek the minimum changes in the original stiffness matrix to match accurately the measured modes and frequencies.[2–8] Once the optimal matrix updates are computed, a second step is necessary to correlate the matrix updates to physically meaningful structural parameter changes. This step may not be straightforward when several structural members are connected to a finite element node.

Another class of methods are sensitivity-based update methods. These methods start with the derivatives of the eigenvalues and/or eigenvectors to changes in material and physical parameters. These sensitivity coefficients are then used to calculate changes in the parameters that would force the analysis frequencies and modes to match those measured in a test.[9] Various optimization techniques can be used to converge on near-optimal solutions. These methods generally require considerable computational expenses. For model refinement, the first-order approximation in computing eigenvalues and eigenvectors works properly since the changes in structural parameters from the initial model to the refined model may be small. For damage detection, this first-order approximation may be inaccurate since a large parameter change due to damage needs to be detected. Consequently, the sensitivity-based approach using the first-order approximation is inadequate for damage detection.

Control system designers have traditionally used eigenstructure assignment techniques to force a structure to respond in a predetermined way. For model refinement and damage location, the desired eigenstructure, i.e., eigenvalues and eigenvectors, is the one that is measured in the test. Minas and Inman[10] and Zimmerman and Widengren[11] have derived methods that determine the pseudo- (fictitious) controller required to produce the test eigenstructure. The control gains can then be translated into matrix adjustments applied to the initial finite element model. Zimmerman and Kaouk[12] applied this eigenstructure model refinement algorithm to structural damage detection. A major difficulty associated with Zimmerman and Kaouk's approach is that the method identifies matrix coefficients changes and thus requires an additional step of identifying structural members corresponding to the changes. This additional step will not be straightforward for complicated spacecraft structures. Also, the method requires a solution of a generalized algebraic Riccati equation, and an iterative solution is proposed to preserve the load path of the undamaged structure, i.e., to maintain the zero–nonzero pattern of the undamaged stiffness matrix. When a structural member is completely damaged, an initial load path is broken. Thus, preserving the load path for damage detection may not be valid for damage cases of entire loss of stiffness.

To perform the system health monitoring, structural health along with sensor and actuator malfunction must be monitored. As a step toward developing a system health monitoring scheme, this research investigates structural damage detection using a constrained eigenstructure assignment. The eigenstructure assignment is selected for the investigation since it may be used not only to perform structural damage detection but also to monitor the sensor and actuator performance in a unified manner. The constrained eigenstructure assignment makes it possible that the computed feedback gains correspond directly to the structural parameter changes without enforcing the zero–nonzero pattern of the initial stiffness matrix. Thus, detection of both partial and complete loss of stiffness is possible, and the additional step of correlating matrix coefficient changes to structural parameter changes is avoided. Also, the proposed approach requires neither a solution of algebraic Riccati equation nor iteration to converge to a solution.

Received Sept. 10, 1993; revision received May 11, 1994; accepted for publication Sept. 14, 1994.

*Assistant Professor, Department of Aerospace Engineering. Member AIAA.

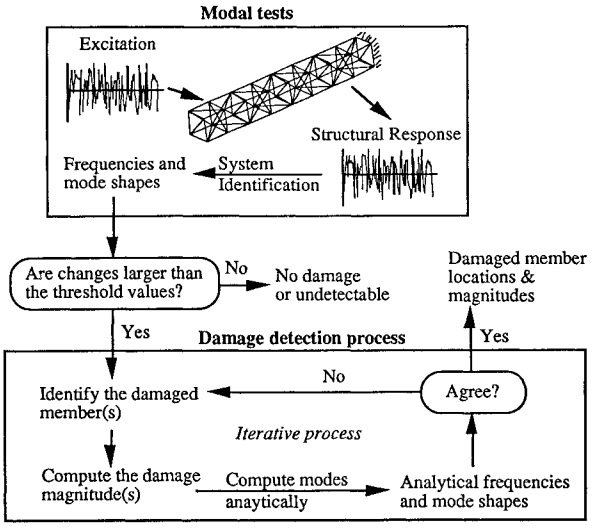

Fig. 1 Damage detection process.

The overview of the damage detection process employed in this paper is shown in Fig. 1. Modal tests are conducted periodically and eigenvalues and eigenvectors (frequencies and mode shapes) are measured to monitor changes in measured modes. When the changes are significant, i.e., larger than the usual measurement uncertainty level, the damage detection process is initiated. Otherwise, the structure is assumed to be healthy or the damage, if exists, is undetectable. In the damage detection process, the measured eigenvalues and eigenvectors are treated as "desired" eigenvalues and eigenvectors for the eigenstructure assignment algorithm to achieve using a feedback control. The location of damage is first identified and the magnitude is estimated. Then, the frequencies and mode shapes of the damaged structure are computed reflecting the location and magnitude of damage. If the analytical modes agree with the test modes within measurement accuracy, the damage detection process is completed. Otherwise, the process will continue until all the damaged struts are identified.

To demonstrate the capability of the approach, a 20-bay planar truss structure is employed. Modal tests are performed using 11 accelerometers for the undamaged structure and several missing member damage cases. Then the test data are used to locate the missing member. The results of damage detection are presented.

Location of Structural Damage

The equation of motion governing the response of an n-DOF (degree-of-freedom) structural system is represented as

$$\boldsymbol{M}\ddot{\boldsymbol{x}} + \boldsymbol{D}\dot{\boldsymbol{x}} + \boldsymbol{K}\boldsymbol{x} = \boldsymbol{F}\boldsymbol{u} \tag{1}$$

where $\boldsymbol{M}$, $\boldsymbol{D}$, and $\boldsymbol{K}$ are the $n \times n$ system mass, proportional damping, and stiffness matrices, respectively; $\boldsymbol{x}$ is a physical displacement vector; $\boldsymbol{u}$ is a $p \times 1$ vector of control forces; and $\boldsymbol{F}$ is an $n \times p$ control influence matrix. Finite element analysis is often used to generate this discretized analytical model of the system. The undamped eigenvalue problem associated with Eq. (1) becomes

$$\left(\lambda_i^2 \boldsymbol{M} + \boldsymbol{K}\right)\phi_i = 0 \qquad \text{for} \qquad i = 1, 2, \ldots \tag{2}$$

where λ_i and ϕ_i are the ith eigenvalue and eigenvector, respectively.

For a typical modal test, a limited number of transducers (e.g., accelerometers) are used. Thus, measured mode shapes are available only at the test DOF, where transducers are placed. The size of the test DOF is typically much smaller than that of the finite element DOF. To provide compatibility in size between the test and analysis mode shapes, either the test mode shapes are expanded[4,12] or the system matrices are reduced,[13] at the expense of losing accuracy. This loss of accuracy can create serious difficulty in performing damage location. The best achievable eigenvector concept[14,15] is employed in this paper to perform the expansion of test mode shapes.

For the purpose of illustrating the constrained eigenstructure assignment approach, consider the mass–spring system shown in Fig. 2a. The system mass and stiffness matrices are defined as

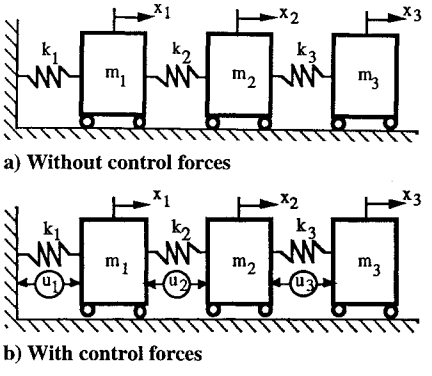

Fig. 2 Mass–spring system.

$$\boldsymbol{M} = \begin{bmatrix} m_1 & 0 & 0 \\ 0 & m_2 & 0 \\ 0 & 0 & m_3 \end{bmatrix}$$

$$\boldsymbol{K} = \begin{bmatrix} k_1 + k_2 & -k_2 & 0 \\ -k_2 & k_2 + k_3 & -k_3 \\ 0 & -k_3 & k_3 \end{bmatrix} \tag{3}$$

with

$$\boldsymbol{x} = \{x_1\ x_2\ x_3\}^T \tag{4}$$

Parallel to the springs, active control forces are added, as shown in Fig. 2b. Then, the $\boldsymbol{F}$ matrix in Eq. (1) becomes

$$\boldsymbol{F} = \begin{bmatrix} 1 & -1 & 0 \\ 0 & 1 & -1 \\ 0 & 0 & 1 \end{bmatrix} \tag{5}$$

with

$$\boldsymbol{u} = \{u_1\ u_2\ u_3\}^T \tag{6}$$

The added control forces represent the force differentials generated due to the loss of stiffness caused by structural damage. The control influence matrix plays an important role in the eigenstructure assignment process since it provides constraints in computing feedback gains that are physically meaningful for structural damage detection.

Since the control forces represent changes in stiffness properties, consider a displacement output feedback control with collocated sensors and actuators as

$$\boldsymbol{u} = -\boldsymbol{G}\boldsymbol{y} \tag{7}$$

where $\boldsymbol{G}$ is a gain matrix and $\boldsymbol{y}$ is a vector containing output feedback variables. Relative displacement measurement becomes

$$\boldsymbol{y} \equiv \boldsymbol{d} = \boldsymbol{F}^T\boldsymbol{x} \tag{8}$$

where $\boldsymbol{d}$ is a relative displacement vector. From Eqs. (7) and (8), the control force becomes

$$\boldsymbol{u} = -\boldsymbol{G}\boldsymbol{F}^T\boldsymbol{x} \tag{9}$$

Substitute the control force in Eq. (9) into the equation of motion (1) and rearrange to obtain

$$\boldsymbol{M}\ddot{\boldsymbol{x}} + \boldsymbol{D}\dot{\boldsymbol{x}} + (\boldsymbol{K} + \boldsymbol{F}\boldsymbol{G}\boldsymbol{F}^T)\boldsymbol{x} = 0 \tag{10}$$

The gain matrix pre- and postmultiplied by the control influence matrix is used to modify the system stiffness matrix. The control influence matrix $\boldsymbol{F}$ plays a role of redistributing the gain matrix to appropriate finite element DOF. Assume that the gain matrix is

diagonal. Then the changes in the stiffness matrix due to control force j, which corresponds to structural member j, can be written as

$$\Delta \boldsymbol{K}_j = \boldsymbol{F}_j g_j \boldsymbol{F}_j^T = g_j \boldsymbol{F}_j \boldsymbol{F}_j^T \tag{11}$$

where $\boldsymbol{F}_j$ is the jth column of $\boldsymbol{F}$ and g_j is the jth diagonal element of $\boldsymbol{G}$. Each diagonal element of the gain matrix represents the change in the corresponding spring stiffness coefficient.

For the type of truss structure used in this investigation, the changes in mass and damping properties due to the removal of a strut were not significant. Thus, changes in mass and damping properties due to damage are not considered in this paper. However, using displacement and velocity feedback simultaneously, the changes in both stiffness and damping properties can be identified.[16] By considering an acceleration feedback, the changes in mass properties may also be identified. Further investigation is needed to be able to detect changes in mass, damping, and stiffness properties simultaneously.

The gain matrix is now obtained to match the measured eigenvalues and eigenvectors. Consider the eigenvalue problem associated with Eq. (10) as

$$\left[\lambda_i^{d^2}\boldsymbol{M} + \lambda_i^d \boldsymbol{D} + (\boldsymbol{K} + \boldsymbol{F}\boldsymbol{G}\boldsymbol{F}^T)\right]\boldsymbol{\phi}_i^d = 0 \tag{12}$$

where λ_i^d and $\boldsymbol{\phi}_i^d$ are the ith desired eigenvalue and eigenvector. They are the measured eigenvalue and eigenvector from the test. Consider the jth structural member and rearrange Eq. (12) as

$$\boldsymbol{\phi}_i^d = \left(\lambda_i^{d^2}\boldsymbol{M} + \lambda_i^d \boldsymbol{D} + \boldsymbol{K}\right)^{-1} \boldsymbol{F}_j \boldsymbol{F}_j^T \left(-g_j \boldsymbol{\phi}_i^d\right) \tag{13}$$

Define

$$\boldsymbol{L}_{ij} \equiv \left(\lambda_i^{d^2}\boldsymbol{M} + \lambda_i^d \boldsymbol{D} + \boldsymbol{K}\right)^{-1} \boldsymbol{F}_j \boldsymbol{F}_j^T \tag{14}$$

$$\eta_{ij}^d \equiv -g_j \boldsymbol{\phi}_i^d \tag{15}$$

to obtain, from Eq. (13),

$$\boldsymbol{\phi}_i^d = \boldsymbol{L}_{ij} \eta_{ij}^d \tag{16}$$

Equation (16) indicates that the desired eigenvector $\boldsymbol{\phi}_i^d$ must reside in the subspace spanned by the columns of $\boldsymbol{L}_{ij}$. The desired eigenvector typically does not precisely reside in the subspace due to modeling and measurement errors. In this case, the eigenvector that is as close as possible, in the least-squares sense, to the desired eigenvector can be computed as[14,15]

$$\boldsymbol{\phi}_{ij}^a = \mathbf{L}_{ij} \mathbf{L}_{ij}^{+} \boldsymbol{\phi}_i^d \tag{17}$$

where $\boldsymbol{\phi}_{ij}^a$ is referred to as the best achievable eigenvector and the superscript plus indicates a pseudoinverse.

Figure 3 illustrates the relationship between the vectors $\boldsymbol{\phi}_{ij}^a$ and $\boldsymbol{\phi}_i^d$ as well as the subspace spanned by the columns of $\boldsymbol{L}_{ij}$. If the measured vector $\boldsymbol{\phi}_i^d$ already lies in the subspace $\boldsymbol{L}_{ij}$, i.e., the damage is caused by the jth structural member, then $\boldsymbol{\phi}_{ij}^a$ and $\boldsymbol{\phi}_i^d$ will be identical. If the damage is caused by a different element or the damage is not reflected in mode i, the two vectors will be different. If $\boldsymbol{\phi}_{ij}^a$ is computed for all structural members that could possibly have caused the damage and the angle between $\boldsymbol{\phi}_{ij}^a$ and $\boldsymbol{\phi}_i^d$ is computed, the damaged element will be indicated by (in the case of perfect data) a zero angle between the two vectors. All others will have

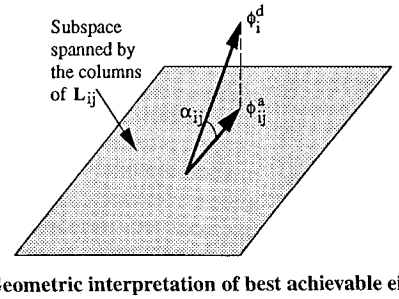

Fig. 3 Geometric interpretation of best achievable eigenvector.

nonzero values. The angle in degrees between the two vectors can be computed as

$$\alpha_{ij} = \frac{180}{\pi} \cos^{-1}\left(\frac{\boldsymbol{\phi}_{ij}^{a^T} \boldsymbol{\phi}_i^d}{\|\boldsymbol{\phi}_{ij}^a\|_F \|\boldsymbol{\phi}_i^d\|_F}\right) \tag{18}$$

where $\|\cdot\|_F$ represents the Frobenius norm. For a structure that has r measured modes and e structural members that could possibly have caused the damage, an $r \times e$ matrix of α can be constructed as

$$\hat{\boldsymbol{A}} = \begin{bmatrix} \alpha_{11} & \alpha_{12} & \cdots & \alpha_{1j} & \cdots & \alpha_{1e} \\ \vdots & \vdots & \ddots & \vdots & \ddots & \vdots \\ \alpha_{i1} & \alpha_{i2} & \cdots & \alpha_{ij} & \cdots & \alpha_{ie} \\ \vdots & \vdots & \ddots & \vdots & \ddots & \vdots \\ \alpha_{r1} & \alpha_{r2} & \cdots & \alpha_{rj} & \cdots & \alpha_{re} \end{bmatrix} \tag{19}$$

If damage is located in structural element j and this damage affects only mode i significantly so that the change in the frequency is measurable, then α_{ij} will be equal or close to zero. All other coefficients will be populated with nonzero entries. Therefore, the location of damage can be identified by searching for a value that is considerably smaller than others in the matrix.

In general, eigenvectors are not available for the entire system DOF. In this case, partition the desired eigenvector as follows:

$$\boldsymbol{\phi}_i^d = \begin{Bmatrix} \boldsymbol{v}_i \\ \boldsymbol{w}_i \end{Bmatrix} \tag{20}$$

where $\boldsymbol{v}_i$ is the specified (measured) portion of the eigenvector and $\boldsymbol{w}_i$ is the unspecified portion. The best achievable eigenvector is then defined, using Eq. (17), as

$$\hat{\boldsymbol{\phi}}_{ij}^a = \boldsymbol{L}_{ij} \hat{\boldsymbol{L}}_{ij}^{+} \boldsymbol{v}_i \tag{21}$$

where $\hat{\boldsymbol{L}}_{ij}$ is the partition of the matrix $\boldsymbol{L}_{ij}$ containing the rows corresponding to $\boldsymbol{v}_i$. In this case, the angle in Eq. (18) is defined as

$$\hat{\alpha}_{ij} = \frac{180}{\pi} \cos^{-1}\left(\frac{\bar{\boldsymbol{\phi}}_{ij}^{a^T} \boldsymbol{v}_i}{\|\bar{\boldsymbol{\phi}}_{ij}^a\|_F \|\boldsymbol{v}_i\|_F}\right) \tag{22}$$

where $\bar{\boldsymbol{\phi}}_{ij}^a$ is the partition of the vector $\hat{\boldsymbol{\phi}}_{ij}^a$ corresponding to the measured portion of the eigenvector.

The best achievable eigenvector serves two purposes: 1) it allows partial specification of the eigenvector and 2) measurement errors that are not consistent with the analytical model are filtered out.[15] The best achievable eigenvector for mode i provides an alternative means of computing the "subspace rotation," as discussed in Ref. 17. The main difference is that the method in Ref. 17 identifies those DOFs that are affected by damage, whereas the method in this paper identifies directly the structural element that is damaged.

Magnitude of Structural Damage

Now the locations of damaged members are identified. The eigenstructure assignment is employed here to compute the feedback gains, i.e., the magnitude of structural damage. Rewrite the equation of motion (1) in state-space form as

$$\dot{\boldsymbol{s}} = \boldsymbol{A}\boldsymbol{s} + \boldsymbol{B}\hat{\boldsymbol{u}} \tag{23}$$

where

$$\boldsymbol{s} = \begin{Bmatrix} \boldsymbol{x} \\ \dot{\boldsymbol{x}} \end{Bmatrix} \qquad \boldsymbol{A} = \begin{bmatrix} \boldsymbol{0} & \boldsymbol{I} \\ -\boldsymbol{M}^{-1}\boldsymbol{K} & -\boldsymbol{M}^{-1}\boldsymbol{D} \end{bmatrix}$$

$$\boldsymbol{B} = \begin{bmatrix} \boldsymbol{0} \\ \boldsymbol{M}^{-1}\hat{\boldsymbol{F}} \end{bmatrix} \tag{24}$$

The matrix $\hat{F}$ contains only those columns corresponding to the damaged members. The output equation (8) then becomes

$$\hat{y} = Cs \equiv [\hat{F}^T\ 0]s \tag{25}$$

The output feedback is thus defined as

$$\hat{u} = -G\hat{y} = -GCs \tag{26}$$

Now the task is to find the diagonal gain matrix G to assign the desired (measured) eigenvalue λ_i^d and eigenvector v_i. The best achievable eigenvectors are written using Eq. (23) and the desired eigenvalues and eigenvectors as

$$v_i^a = L_i \hat{L}_i^+ v_i \tag{27}$$

where $L_i = (\lambda_i^d I - A)^{-1}B$ and $\hat{L}_i \equiv$ rows in upper half of L_i corresponding to measurement DOF employed in v_i. Using the constrained eigenstructure assignment algorithm by Andry et al.,[14] the jth diagonal gain of G is computed as

$$g_j = -\Psi_j \Omega_j^+ \tag{28}$$

where Ψ_j is the jth row of Ψ and Ω_j is the jth row of Ω. In the above equation, the matrices Ψ and Ω are defined as

$$\Omega \equiv \hat{C}V \qquad \Psi \equiv Z - A_1 V \tag{29}$$

where $\hat{C}$ is a transformed C matrix, V a matrix of transformed best achievable eigenvectors, Z the partition of a matrix that is a product of desired eigenvalues and V, and A_1 the partition of a transformed A matrix. Thorough derivation of Eq. (28) is available in Ref. 14. The diagonal gain g_j in Eq. (28) corresponds to the stiffness change of the jth structural member, i.e., the magnitude of structural damage, that satisfies the measured eigenvalues and eigenvectors in the least-squares sense. Due to inaccuracy in measured modes and the analytical model, the magnitude of structural damage will not be exact.

Some of the desirable features of the approach described above include the following: 1) it updates the physical structural elements directly instead of updating matrix coefficients, which may or may not be physically realizable, 2) measured mode shapes are not required for the entire finite element DOF, and 3) it requires neither a solution of algebraic Riccati equation nor iteration to converge to a solution compared to the other eigenstructure assignment based damage detection method.

Detection of Multiple Damage

When there are more than one damaged element in the structure, the examination of the matrix $\hat{A}$ in Eq. (19) may not provide a clear indication of the damaged members. If the matrix $\hat{A}$ does not indicate the damaged member clearly, it may imply that there are multiple damaged members. To examine multiple damage, a sequential damage detection approach is employed. In this approach, damaged members are identified one at a time in an iterative process until all the damaged members are identified, as indicated in Fig. 1. The first step of the approach is to select the single most probable damaged member by examining the $\hat{A}$ matrix. Next, the magnitude of damage of the member is computed using Eq. (28). Then, the undamaged stiffness matrix is modified to reflect the stiffness matrix change corresponding to the damaged member. For instance, if strut k has been identified as a damaged member and the corresponding feedback gain (g_k), i.e., stiffness loss, is computed, the undamaged stiffness matrix will be modified using Eqs. (10) and (11) as

$$K_{\text{new}} = K + g_k F_k F_k^T \tag{30}$$

where the matrix K_{new} is the new undamaged stiffness matrix and F_k is the kth column of F.

Then, the new undamaged stiffness matrix is used to compute the new best achievable eigenvectors in Eq. (21) and a new $\hat{A}$ matrix in Eq. (19). Again, another single most probable damaged member is selected using the new $\hat{A}$ matrix. This iterative process is continued until all the damaged members are located. At the end of each iteration, the natural frequencies are computed using the new undamaged matrix and compared with those of measured frequencies. When the differences are small, i.e., within the usual error bound of a modal test, the iteration terminates. This comparison also can be used to ascertain whether the selected member is indeed responsible for the damage.

Damage Detection of Twenty-Bay Planar Truss Structure

The 20-bay planar truss shown in Fig. 4 is used in implementing the damage detection method described above. The diagonal and side dimensions of each square bay are 0.5 and 0.354 m, respectively. The truss is constructed from aluminum truss members, steel joints, and transverse steel bars. The truss is oriented in a horizontal plane with its weight supported by steel balls on table tops. More information on the truss is available in Ref. 18.

For the damage detection studies, the truss is modeled using a rod element (axial stiffness only) per strut and lumped masses for the joints and steel bars. So the system has 2 DOF per node, resulting in 80 system DOF. The first four natural frequencies of the truss are shown in Table 1 in comparison to the test results. For modal tests, the truss was instrumented with 11 single-axis accelerometers, as indicated in Fig. 4. A shaker was mounted at the free end of the truss to provide excitation for modal tests. The first mode frequency is not consistent and varies widely (1.8–2.2 Hz) from test to test. This lack of consistency poses difficulty in detecting the longeron damage cases, as will be discussed later. The large error in the first mode frequency is contributed partly by the friction of the balls, which is not modeled in the analysis, the low-frequency inaccuracy of the transducers, and the modal test setup, which was designed to measure all four mode simultaneously.

Four damage cases shown in Table 2 are investigated, including missing longerons and diagonals. The batten damage cases are not studied since the batten stiffness is dominated by the steel bars and the axial mode is not measured. All the longerons and diagonals are considered as damage candidates. Thus, the size of the F matrix in Eq. (1) becomes 80 (DOF) by 60 (damage candidates). The F matrix is easily defined by replacing each strut with an axial control force and considering the location and direction of the control force. The measured frequencies for the damage cases are summarized in Table 3. Among the 11 test DOF available, 10 test DOF were selected to perform damage detection. The test DOF at the free end of the truss was not used.

Figure 5 shows the results of damage location for damage case A. The angles are computed using Eq. (22). The smaller the angle is, the

Table 1 First four bending frequencies of undamaged planar truss

Mode number	Analytical frequency, Hz	Test frequency, Hz	Description
1	1.60	1.80 to 2.20	First bending mode
2	9.36	9.35	Second bending mode
3	24.70	24.21	Third bending mode
4	43.23	42.74	Fourth bending mode

Table 2 Damage cases investigated for planar truss

Damage case	Damaged strut	Damage condition
A	Upper longeron in bay 2	Strut out
B	Lower longeron in bay 7	Strut out
C	Diagonal in bay 9	Strut out
D	Diagonal in bay 14	Strut out

Table 3 Measured natural frequencies due to damage (Hz)

Damage case	Mode 1	Mode 2	Mode 3	Mode 4
A	1.27	8.00	22.00	42.56
B	0.85	8.06	17.00	42.11
C	2.07	9.41	20.80	37.39
D	2.22	9.31	23.71	29.86

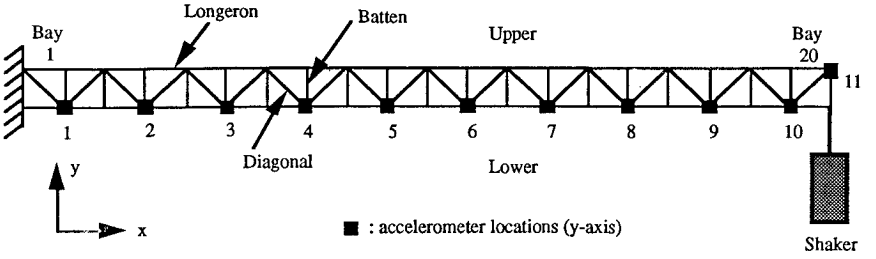

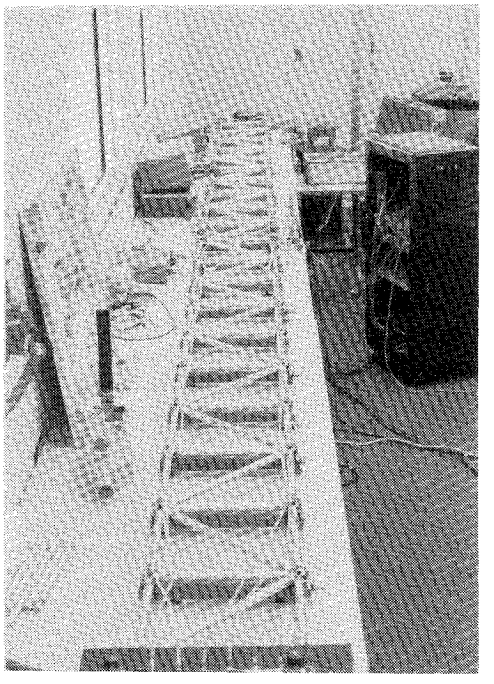

Fig. 4 Twenty-bay planar truss structure used for damage detection.

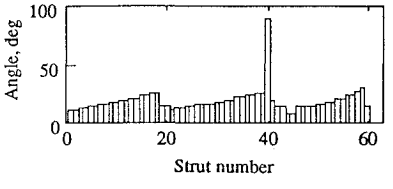

a) Obtained using mode 1

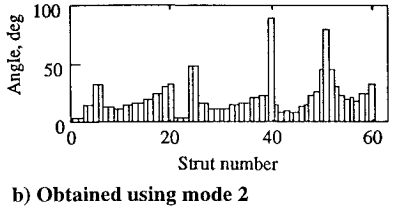

b) Obtained using mode 2

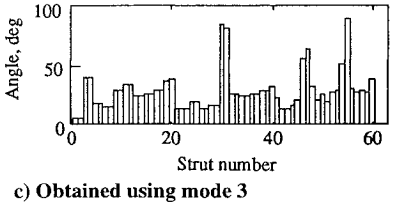

c) Obtained using mode 3

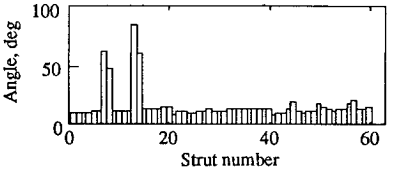

d) Obtained using mode 4

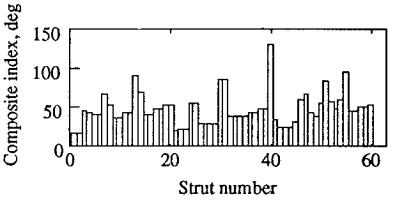

e) Obtained using modes 1, 2, 3, and 4

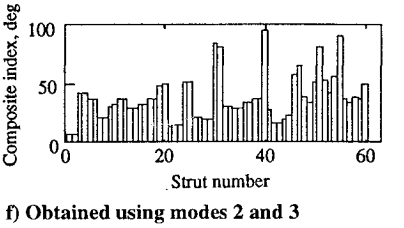

f) Obtained using modes 2 and 3

Fig. 5 Damage location results of damage case *A*.

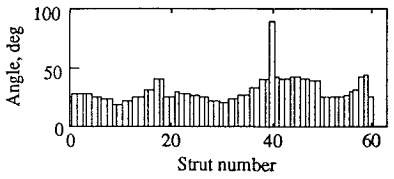

a) Obtained using mode 1

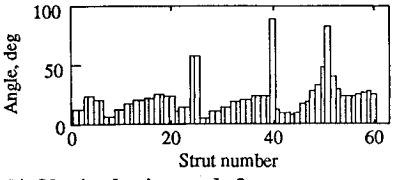

b) Obtained using mode 2

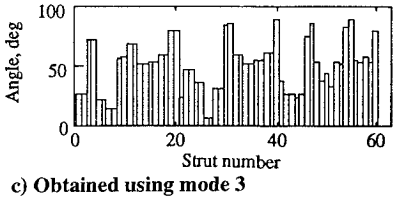

c) Obtained using mode 3

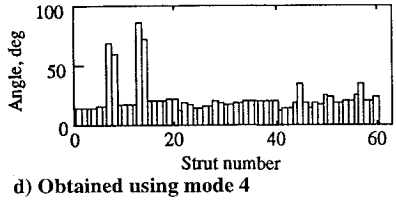

d) Obtained using mode 4

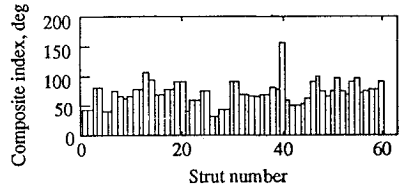

e) Obtained using modes 1, 2, 3, and 4

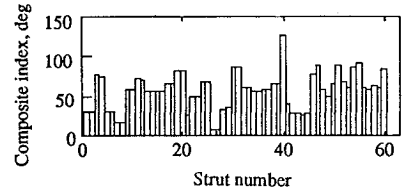

f) Obtained using modes 2 and 3

Fig. 6 Damage location results of damage case *B*.

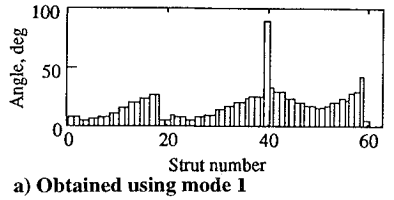

a) Obtained using mode 1

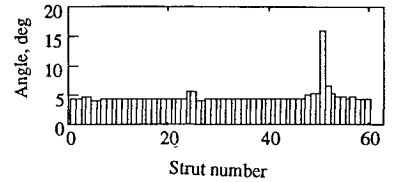

b) Obtained using mode 2

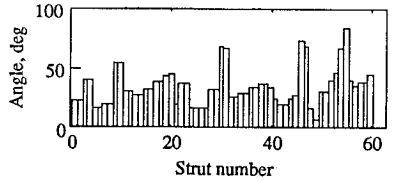

c) Obtained using mode 3

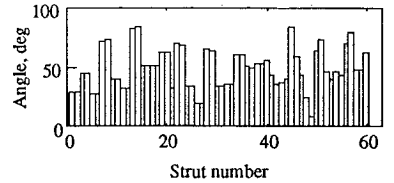

d) Obtained using mode 4

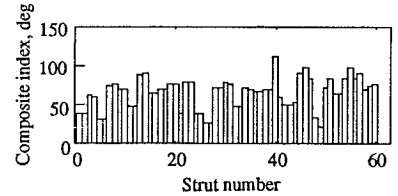

e) Obtained using modes 1, 2, 3, and 4

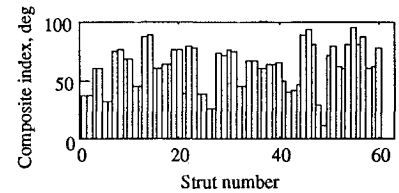

f) Obtained using modes 3 and 4

Fig. 7 Damage location results of damage case *C*.

more chance there is for damage. In the figure, strut numbers 1–20 correspond to the upper longerons from bay 1 to bay 20 and numbers 21–40 correspond to the lower longerons. The strut numbers from 41 to 60 correspond to diagonals from bay 1 to bay 20. The angles obtained using mode 1 are not accurate because of the measurement inaccuracy in mode 1. Since the damage on longerons tends to create large changes in the lower bending modes, this lack of measurement accuracy of mode 1 makes the damage location difficult. The angles obtained using mode 4 do not provide meaningful information since the frequency change in mode 4 is very small for damage case *A*, as indicated in Tables 1 and 3. Modes 2 and 3 provide consistent information, and it can be seen that struts 1 and 2 consistently produce the smallest angles. Therefore, we can conclude that the damage occurred either in upper longeron 1 or 2.

Measurement error and the small number of test DOF (10 DOF compared to 80 finite element DOF) make the angles contaminated, as shown in Figs. 5–8. Instead of examining angles computed using each mode at a time, a single composite index is proposed to help locate the damaged number. The jth composite index, which represents the Euclidean distance of angles produced by the measured modes for member j, is defined as

$$a_j = \|\hat{\boldsymbol{A}}_j\|_F \tag{31}$$

where $\hat{\boldsymbol{A}}_j$ is the jth column of $\hat{\boldsymbol{A}}$ in Eq. (19). Figures 5e and 5f show the composite indices using modes 1–4 and modes 2 and 3, respectively. The composite index helps clarify the damaged members.

Due to the lacing pattern of the diagonals in the planar truss, which is a V shape, the changes in modes created by the upper longerons in bays 1 and 2 are almost identical. This is true for all the pairs consisted of upper longerons in bays 3 and 4, 5 and 6, and so on, i.e., the longeron pair at the open end of the V. Therefore,

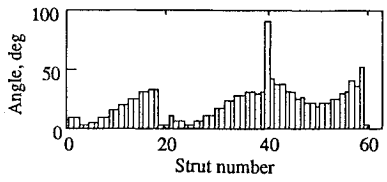

a) Obtained using mode 1

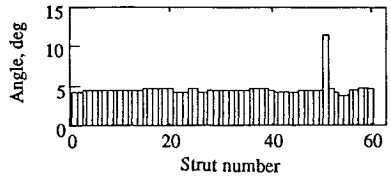

b) Obtained using mode 2

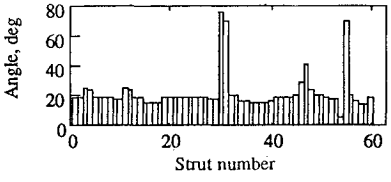

c) Obtained using mode 3

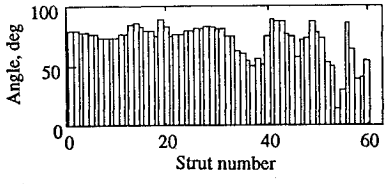

d) Obtained using mode 4

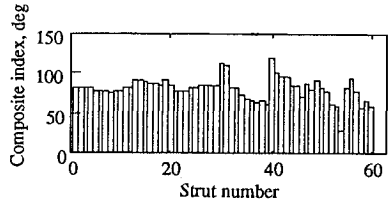

e) Obtained using modes 1, 2, 3, and 4

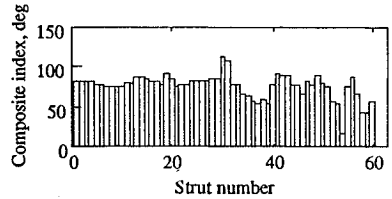

f) Obtained using modes 3 and 4

Fig. 8 Damage location results of damage case *D*.

this unique situation makes it practically impossible to single out the damaged longeron.

The situation is similar for the lower longeron damage case *B*. The lower longeron pairs 2 and 3, 4 and 5, and so on, produce almost identical changes in modes. Results of damage case *B* are shown in Fig. 6. Again, due to the measurement inaccuracy in mode 1 and the insignificant frequency change in mode 4, the angles obtained using modes 1 and 4 do not provide meaningful information. Modes 2 and 3 indicate that either strut number 26 (lower longeron 6) or strut number 27 (lower longeron 7) is damaged. The composite index using modes 2 and 3 helps clarify the damaged members.

Figures 7 and 8 show the results of damage location for damage cases *C* and *D*, respectively. The angles obtained using mode 1 are not accurate because of the measurement inaccuracy in mode 1. The second mode frequency is not affected much by the damage since the damage on diagonals tends to create large changes in the higher bending modes, as indicated in Table 3. Therefore, the angles obtained using mode 2 do not provide meaningful information. Modes 3 and 4 provide consistent information, and it can be seen that strut 49 for damage case *C* and strut 54 for damage case *D* consistently produce the smallest angles and composite indices. Therefore, we can conclude that the damage occurred in the diagonals in bays 9 and 14 for damage cases *C* and *D*, respectively. Unlike the longeron damage cases, the damage diagonals can be identified uniquely. Since the location of damaged is known, the magnitude of damage can be computed using Eq. (28). The constrained gains computed using modes 3 and 4 are −58,825 and −59,666 for damage cases *C* and *D*, respectively. Considering that the effective axial stiffness of the undamaged diagonal is 61,673 lb/in., the method accurately predicts, within 5% error, the amount of stiffness loss due to the missing diagonal.

Concluding Remarks

A systematic approach to locating structural damage using a refined analytical model of the undamaged structure and measured modes was developed and demonstrated using the 20-bay planar truss. This approach first locates the damage using the concept of best achievable eigenvectors and then identifies the magnitude of damage using a constrained eigenstructure assignment. Instead of identifying the changes in the stiffness matrix for damage location, as most of the currently available methods do, the approach locates the damaged element directly. Thus, the additional step of locating damaged members from the stiffness matrix changes is avoided. As demonstrated in the planar truss example, the method does not require full finite element DOF mode shapes. The instrumented DOF can be much smaller than the finite element DOF (10 DOF out of 80 finite element DOF for the example). Thus the burden of using a large number of transducers for damage detection is relieved. Once the location of damage is known, the magnitude of damage can be accurately computed using the constrained eigenstructure assignment method.

As was revealed by the planar truss example, the approach has its limitations. The limitations mainly stem from the measurement error in mode shapes and frequencies. As the test data get inaccurate, the damage location can be blurred significantly. A judicious selection of test modes may be critical in performing a successful damage detection. Also, each individual damage case must be able to produce a unique pattern of change in frequencies and mode shapes. Otherwise, as indicated in the planar truss longeron damage cases, pinpointing the damaged member may not be feasible.

Due to the nature of the truss structure employed in this study, damping and mass property changes due to damage were ignored. Incorporation of velocity and acceleration feedback gains will allow simultaneous detection of mass, damping, and stiffness losses. Further investigation in this respect needs to be conducted.

Acknowledgments

This research was supported by the Air Force Office of Scientific Research through the Summer Faculty Research Program at the Frank J. Seiler Research Laboratory at the U.S. Air Force Academy. This investigation was also supported in part by the University of Kansas General Research Allocation 3033-X0-0038. The author is grateful for the supports in the laboratory from Daniel Stech, Jeffrey Turcott, and Jeffrey Kouri.

References

[1]Hanks, B. R., "Dynamics Challenges for 21st Century Spacecraft," Keynote Address, 61st Shock and Vibration Symposium, Pasadena, CA, Oct. 1990.

[2]Brock, J. E., "Optimal Matrices Describing Linear Systems," *AIAA Journal*, Vol. 6, No. 7, 1968, pp. 1292–1296.

[3]Baruch, M., "Optimal Correction of Mass and Stiffness Matrices Using Measured Modes," *AIAA Journal*, Vol. 20, No. 11, 1982, pp. 1623–1626.

[4]Berman, A., and Nagy, E. J., "Improvement of a Large Analytical Model Using Test Data," *AIAA Journal*, Vol. 21, No. 8, 1983, pp. 1168–1173.

[5]Kabe, A. M., "Stiffness Matrix Adjustment Using Mode Data," *AIAA Journal*, Vol. 23, No. 9, 1985, pp. 1431–1436.

[6]Kammer, D. C., "Optimal Approximation for Residual Stiffness in Linear System Identification," *AIAA Journal*, Vol. 26, No. 1, 1988, pp. 104–112.

[7]Smith, S. W., and Beattie, C. A., "Secant-Method Matrix Adjustment for Structural Models," *AIAA Journal*, Vol. 29, No. 1, 1991, pp. 119–126.

[8]Smith, S. W., and Hendricks, S. L., "Damage Detection and Location in Large Space Trusses," *AIAA SDM Issues of the International Space Station, A Collection of Technical Papers*, AIAA, Washington, D.C., 1988, pp. 56–63.

[9]Collins, J. D., Hart, G. C., Hasselman, T. K., and Kennedy, B., "Statistical Identification of Structures," *AIAA Journal*, Vol. 12, No. 2, 1974, pp. 185–190.

[10]Minas, C., and Inman, D. J., "Matching Finite Element Models to Modal Data," *Journal of Vibration and Acoustics*, Vol. 112, No. 1, 1990, pp. 84–92.

[11]Zimmerman, D. C., and Widengren, W., "Correcting Finite Element Models Using a Symmetric Eigenstructure Assignment Technique," *AIAA Journal*, Vol. 28, No. 9, 1990, pp. 1670–1676.

[12]Zimmerman, D. C., and Kaouk, M., "Eigenstructure Assignment Approach for Structural Damage Detection," *AIAA Journal*, Vol. 30, No. 7, 1992, pp. 1848–1855.

[13]Lim, T. W., "A Submatrix Approach to Stiffness Matrix Correction Using-Modal Test Data," *AIAA Journal*, Vol. 28, No. 6, 1990, pp. 1123–1130.

[14]Andry, A. N., Shapiro, E. Y., and Chung, J. C., "Eigenstructure Assignment for Linear Systems," *IEEE Transactions on Aerospace and Electronic Systems*, Vol. AES-19, No. 5, 1983, pp. 711–729.

[15]Lim, T. W., and Kashangaki, T. A.-L., "Structural Damage Detection of Space Truss Structures Using Best Achievable Eigenvectors," *AIAA Journal*, Vol. 32, No. 5, 1994, pp. 1049–1057.

[16]Lim, T. W., "Characterization of Passively Damped Struts Using a Constrained Eigenstructure Assignment," *Proceedings of the AIAA/ASME/ASCE/AHS/ASC Structures, Structural Dynamics, and Materials Conference*, Pt. 5, AIAA, Washington, DC, 1994, pp. 2644–2654; also AIAA Paper 94-1650.

[17]Zimmerman, D. C., and Kaouk, M., "Structural Damage Detection Using a Subspace Rotation Algorithm," AIAA Paper 92-2521, April 1992.

[18]Hallauer, W. L., and Lamberson, S. E., "A Laboratory Planar Truss for Structural Dynamics Testing," *Experimental Techniques*, Vol. 13, No. 9, 1989, pp. 24–27.